HHS Public Access

Author manuscript

*Exp Eye Res*. Author manuscript; available in PMC 2023 February 01.

Published in final edited form as:

*Exp Eye Res*. 2022 February ; 215: 108902. doi:10.1016/j.exer.2021.108902.

# Altered transsulfuration pathway enzymes and redox homeostasis in inherited retinal degenerative diseases

**Alireza Badiei**[1,2], **William A Beltran**[2], **Gustavo D Aguirre**[2]

[1]Department of Veterinary Medicine, College of Natural Science and Mathematics, University of Alaska Fairbanks, AK, USA

[2]Division of Experimental Retinal Therapies, Department of Clinical Sciences and Advanced Medicine, School of Veterinary Medicine, University of Pennsylvania, Philadelphia, PA, USA

## Abstract

Retinal degenerative diseases result from apoptotic photoreceptor cell death. As endogenously produced gaseous molecules such as hydrogen sulfide ($H_2S$) and nitric oxide (NO) play a key role in apoptosis, we compared the expression levels of genes and proteins involved in the production of these molecules in the retina of normal dogs and three canine models (rcd1, crd2, and xlpra2) of human inherited retinal degeneration (IRD). Using qRT-PCR, western blot, and immunohistochemistry (IHC), we showed that mRNA and protein levels of cystathionine β–synthase (CBS), an enzyme that produces $H_2S$ in neurons, are increased in retinal degeneration, but those of cystathionine γ-lyase (CSE), an enzyme involved in the production of glutathione (GSH), an antioxidant, are not. Such findings suggest that increased levels of $H_2S$ that are not counterbalanced by increased antioxidant potential may contribute to disease in affected retinas. We also studied the expression of neuronal and inducible nitric oxide synthase (nNOS and iNOS), the enzymes responsible for NO production. Western blot and IHC results revealed increased levels of nNOS and iNOS, resulting in increased NO levels in mutant retinas. Finally, photoreceptors are rich in polyunsaturated fatty acids (PUFAs) that can make these cells vulnerable to oxidative damage through reactive oxygen species (ROS). Our results showed increased levels of acrolein and hydroxynonenal (4HNE), two main toxic products of PUFAs, surrounding the membranes of photoreceptors in affected canines. Increased levels of these toxic products, together with increased NO and ROS, likely render these cells susceptible to an intrinsic apoptotic pathway involving mitochondrial membranes. To assess this possibility, we measured the levels of BCL2, an anti-apoptotic protein in the mitochondrial membrane. Western blot results showed decreased levels of BCL2 protein in affected retinas. Overall, the results of this study identify alterations in the expression of enzymes directly involved in maintaining the normal redox

Correspondence during the review process: Alireza Badiei, Department of Veterinary Medicine, College of Natural Science and Mathematics, University of Alaska Fairbanks, Fairbanks, AK 99775; 9074741968; abadiei@alaska.edu.

Declaration of interest:

The authors report no conflicts of interest. The authors alone are responsible for the content and writing of the paper.

status of the retina during retinal degeneration, thereby supporting future studies to investigate the role of $H_2S$ and NO in retinal degeneration and apoptosis.

**Keywords**

CBS; CSE; NO; ROS; mitochondria; photoreceptor degeneration; retinal degeneration

## Introduction

Mutations in many genes expressed in either the retina or retinal pigment epithelium (RPE) can cause visual disorders, retinal degeneration, and eventually blindness (Aguirre, 2017). The diseases are characterized by photoreceptor cell apoptosis, a type of programmed cell death manifested by morphological and biochemical alterations (Portera-Cailliau et al., 1994). RPE performs a number of functions critical for maintaining retinal homeostasis (Fuhrmann et al., 2014). Impairment of RPE, a scavenger for ROS, will cause excessive oxidative stress and mitochondrial disruption that contribute to retina degeneration (Ao et al., 2018). Mutations in genes expressed in the RPE would bring about photoreceptor degeneration in inherited diseases of the RPE (Donato et al., 2020). Photoreceptor cell apoptosis plays a crucial role in inherited retinal degenerative diseases and light-induced retinal degeneration models (Wenzel et al., 2005; Rajala and Rajala, 2013). Apoptosis can be initiated by either extrinsic or intrinsic pathways (Locksley and Lenardo, 2001), the latter of which is driven by changes in the mitochondria (Wang and Youle, 2009). Mitochondria consume the majority of the total oxygen content in the cell for use in oxidative phosphorylation and cellular ATP production (Brown, 1992) and are the main source for generating reactive oxygen species (ROS). Antioxidant redox systems remove physiological levels of ROS, but excess levels of ROS cause permanent oxidative damage that leads to apoptosis.

The retina is a specialized tissue with a high metabolic rate and a consequently high level of oxygen consumption. These conditions can result in the generation of ROS that renders the retina vulnerable to oxidative damage. The retina is also susceptible to oxidative stress due to a combination of high levels of polyunsaturated fatty acids (PUFAs) in the photoreceptor membrane that is subject to peroxidation—leading to the production of toxic metabolites. In addition, the retina is subject to chronic exposure to light, which leads to increased levels of ROS (Fliesler and Anderson, 1983). Peroxidation of PUFAs and excess levels of ROS can damage membrane proteins in mitochondria and trigger apoptosis through the mitochondria pathway in both RPE and photoreceptors (Sharma et al., 2008; Jarrett et al. 2008). As maintenance of the redox status in the retina is compromised by PUFA peroxidation and excess ROS generation, defense mechanisms to ameliorate these detrimental effects are essential. Glutathione (GSH) is one of the key antioxidant sources in the retina and its level is critical for retinal cell survival; reduced levels of GSH can result in oxidative stress and increased retinal cell death (Roh et al. 2007) while increased levels protect RPE cells against oxidative stress (Liang et al., 2005). Excessive nitric oxide (NO) generation can also promote lipid peroxidation (Siu and To, 2002) and oxidative damage. However, GSH prevents lipid and protein damage induced by NO in the retina (Siu et al., 2015), suggesting

a protective role for GSH against NO-induced retinal toxicity (Haq et al., 2007; Ganea and Harding, 2006) and highlighting the crucial role of antioxidants in protection retinal cells from oxidative damage.

The transsulfuration pathway (TSP) is a methionine metabolic pathway leading to the biosynthesis of cysteine and eventually GSH. Cystathionine β-synthase (CBS) and cystathionine γ-lyase (CSE) are the active enzymes in this pathway, which are also involved in homocysteine (Hcy) homeostasis and $H_2S$ production (Stipanuk, 2004; Singh et al., 2009). Hcy condenses with serine to form cystathionine in a reaction catalyzed by CBS. Then, CSE cleaves cystathionine and releases free cysteine for GSH synthesis (Finkelstein, 1990). CSE plays a key role in this process and the levels of GSH are reduced when the CSE gene is downregulated (Parsanathan and Jain, 2018). Growing evidence suggests that $H_2S$ contributes to a wide range of physiological and pathological functions, including oxidative stress, the cellular stress response, inflammation, and apoptosis (Bhatia, 2012; Badiei et al., 2013; Han et al., 2019; Badiei et al., 2016). Notably, $H_2S$ protects against oxidative damage and apoptosis in the retina (Erisgin et al., 2019), potentially by regulating $Ca^{2+}$ influx (Du and Yang, 2017). However, at high concentrations, $H_2S$ inhibits cytochrome c oxidase in mitochondrial complex IV (Szabo et al., 2014), highlighting its potential pathologic impact. As any changes in mitochondria function can trigger apoptosis, the potential effects of $H_2S$ on mitochondrial function could have a significant impact on the retina. In this study, we used three different canine models of IRD to investigate molecular alterations involved in oxidative stress, apoptosis, and mitochondrial dysfunction. Specifically, we focused on alterations in the expression levels of the main TSP enzymes, NO producing enzymes, levels of lipid metabolites produced following lipid peroxidation as a readout of oxidative damage, and assessment of mitochondria protein levels that reflect the functional integrity of the mitochondria. This information will be important for further investigation of the role of these enzymes in retinal degeneration.

## Material and methods

### Animals

Retinas from normal and diseased dogs were used for this study (Table 1). To study the TSP and redox pathways at the onset and during the course of disease, samples were collected from different age groups. For qPCR and western analyses, the ages selected correspond to the time points following the early peak of cell death (Gardiner et al., 2016; Downs et al., 2016). These time points, as well as an age when there is more advanced degeneration, were also included in the immunohistochemistry (IHC) studies. Three different canine models of IRD were used: xlpra2, an early onset and rapidly progressing model of x-linked retinitis pigmentosa (XLRP) caused by a deletion in PRGR (Zhang et al., 2002), rcd1, an early onset and rapidly progressing model of retinitis pigmentosa caused by a mutation in PDE6B, (Ray et al., 1994), and crd2, a model of Leber congenital amaurosis (LCA) caused by a mutation in NPHP5 (Goldstein et al., 2013). All dogs were housed under identical conditions (diet, ambient illumination with cyclic 12 hrs ON-12 hrs OFF light) at the Retinal Disease Studies (RDS) facility in Kennett Square, Pennsylvania. The study was approved by the Institutional Animal Care and Use Committee (IACUC) of the University of Pennsylvania and strictly

adhered to the ARVO Statement for the Use of Animals in Ophthalmic and Vision Research. To control expression with the time of day, the animals were euthanized, and tissues were collected between 7:30–9:30 am.

### RNA extraction, cDNA synthesis, and qRT-PCR

RNA was purified from neuroretina, and quantitative real-time PCR was performed as described previously (Badiei et al., 2019). All PCR reactions were normalized to the Ct value of GAPDH. Fold change was calculated as $2^{-(\Delta\Delta Ct)}$. The sense and antisense primers for CSE, CBS, NOS2, BCL2, and GAPDH were designed using the PrimerQuest Tool from Integrated DNA Technologies (Table 2).

### Protein extraction and western blot analysis

The neuroretina was homogenized, sonicated, and then centrifuged, and total protein concentration in the supernatant was measured by BCA assay and western blot performed as described previously (Badiei et al., 2019). The ultimate goal for this study was to examine CSE, CBS, BCL2, NOS1 in degenerating retinas. Since the loss of actin and tubulin, two proteins enriched in photoreceptors, may effect the interpretation of expression changes occurring in inner retinal layers with degeneration, GAPDH was used instead as a housekeeping gene. Normalization to GAPDH and analyses were done using Image Studio Software provided by LI-COR (LI-COR, Lincoln, NE).

### Immunodetection of target proteins in intact retinal tissue

Expression and localization of CBS, CSE, NOS1 (nNOS), NOS2 (iNOS), Hydroxynonenal (4HNE), and acrolein were analyzed by immunohistochemistry (IHC) as described previously (Badiei et al., 2019). Sections were stained with primary antibodies at 4 °C overnight (Table 3), and antigen-antibody complexes were visualized with Alexa Fluor® -conjugated secondary antibodies (Invitrogen, Thermo Fisher Scientific). For an illustration of IHC findings, images were digitally captured approximately midpoint between the optic disc and ora serrata using a Spot 4.0 camera with SPOT 4.0 software (SPOT Imaging, Sterling, Heights, MI). For IHC fluorescence microscopy, the same exposures and the image handling procedures were utilized for each set of sections representing control and mutant retinas evaluating a specific antibody.

### Statistics

The fold change in mRNA expression of the target gene was calculated using the $2^{-\Delta\Delta Ct}$ method. Data are expressed as mean ± standard deviation. The unpaired independent t-test, One-way ANOVA, and Tukey's multiple comparison tests were used for statistical analysis using Graph Pad version 8. The experiments were performed in three samples with technical triplicates for each sample, and the results are expressed as mean ± SD. A p-value of $<0.05$ was considered statistically significant.

## Results

To assess the regulation of redox potential in retinal disease and its role in degeneration mechanisms, we examined key genes and proteins belonging to the transsulfuration pathway

and redox homeostasis interactome in three models of canine retinal degeneration (xlpra2, rcd1, and crd2). Figure 1 provides a schematic overview of the pathways examined. Overall, we found that CBS gene and protein levels increased during retinal degeneration while CSE levels remained unchanged. Enhanced levels of toxic metabolites acrolein and 4HNE indicated increased lipid peroxidation of photoreceptors membranes, suggesting oxidative damage to the retina. Finally, affected retinas also showed excessive NO levels and reduced protein levels of BCL2, an anti-apoptotic protein in the mitochondrial membrane. These results are detailed in the following sections.

## CBS and CSE expression in retinal degenerative diseases

qRT-PCR analysis of retinal samples showed that CBS mRNA expression levels increased in rcd1 and crd2 mutant retinas in the 9–14 weeks of age time period (Figure 2a). In contrast, CSE mRNA expression in the diseased retina was comparable to that of normals (Figure 2b). The increased levels of CBS mRNA expression in rcd1 and crdr2 groups suggest alterations in homocysteine homeostasis and the potential increase in $H_2S$ generation that could contribute to the disease process. However, as CSE levels were comparable in normal and diseased retinas, it suggests that the levels of GSH in normal and affected dogs would be equivalent and would therefore not impact disease-induced alteration in redox potential.

CBS western blot analysis of the same retinal samples was evaluated to determine if diseases impacted CBS protein expression. Results were consistent with the mRNA expression results and showed statistically significant increases in CBS protein expression in rcd1 and crd2 (Figure 2c, e). A single protein band of approximately 63 kDa, corresponding to the CBS protein, was found in normal and affected retinas (Figure 2c). Western blot analysis of normal and diseased retinas for the expression of CSE protein confirmed a single-protein band of approximately 43 kDa, but there was no disease-associated change in expression in comparison with control samples (Figure 2d, f). These results further support the potential that increased levels of CBS in affected retinas result in higher levels of $H_2S$ production compared to normal retinas, while comparable levels of CSE protein expression suggest that GSH levels are likely unchanged in mutant retinas.

To examine CBS expression during postnatal development of normal and mutant retinas, IHC studies were performed (Table 1). In normal dogs, CBS expression was observed in the outer segment of the photoreceptor cells, in horizontal cells, and in the ganglion cell layer (GCL) in the fully developed retina. At the earliest time points, CBS staining was detected only in the horizontal cells and GCL (Figure 3). These findings were consistent with our previous study, which localized CBS using markers specific for different cell types in the retina layers (Badiei et al., 2019). CBS expression in young normal and mutant retinas (aged 5 and 12–16 weeks) were comparable (Figure 3). In contrast, CBS expression increased in older mutant retinas compared to normal (aged 24–48 weeks), revealing an age-dependent increase in affected dogs. The increased CBS protein expression was most prominent in the GCL and highest in crd2; as most photoreceptors had degenerated at this more advanced time point, the more prominent outer segment immunolabeling characteristic of older control retinas could not be evaluated in the mutant retinas (Figure 3).

We next examined CSE protein expression changes in normal and mutant retinas by IHC at the same time points (Table 1). CSE was predominantly expressed in inner retinal neurons, especially at an older age, and there were no differences between normal and mutant retinas at five weeks of age (Figure 4). IHC analysis showed that the intensity of CSE staining was higher in the GCL layer in xlpra2 (age: 24–48 weeks) and rcd1 (12–16 weeks) (Figure 4). The labeling intensity for CSE did not increase with aging in normal and affected retinas.

## Alteration in the proteins and molecules involved in oxidative stress

**Increased levels of NOS1 and NOS2 is an indication of increased production of NO in retinal degenerative disease—**At physiologic concentrations, NO is a signaling molecule. However, excessive NO production under pathological conditions results in the formation of reactive nitrogen species and neuronal cell death (Figure 1; Pathway 2). To examine the potential role of NO in these diseases, localization of neuronal NOS1 (nNOS) and inducible NOS2 (iNOS) was performed. At the earliest time points, mutant retinas showed increased immunolabeling in the inner segment (IS) region adjacent to the outer limiting membrane (OLM), as well as increased labeling in the GCL, particularly in xlpra2 and rcd1 dogs (Figure 5a). The increased NOS1 immunolabeling in the IS and OLM region of mutants persisted at the later time points examined (Figure 5a).

IHC showed increased NOS1 expression in the outer limiting membrane (OLM) and GCL in affected retinas compared to normal (Figure 5a). IHC results from 5-week old dogs showed an increase in NOS1 protein expression in the OLM of affected dogs compared to normal. In addition, the 5 and 12-week-old xlpra2 retinas showed increased NOS1 labeling in the INL and inner plexiform layers (Figure 5a D, E). As the immunolabeling intensity was greatest in cells bordering the vitreal aspect of the INL, it is possible that Müller cells accounted for the more diffuse overall labeling found in this model at the two time points. The increased NOS1 suggests that NO production by neurons may be increased in the retinas of affected dogs.

Western blot analysis to examine NOS1 (nNOS) protein expression in normal and mutant retinas showed a significantly higher level of NOS1 in the xlpra2 and rcd1 retinas, with levels of (4.4 ± 1.82) and (5.4 ± 1.53) than in the normal retina, respectively (one-way ANOVA, $p<0.0$) (Figure 5b, c). Increased levels of nNOS expression in the xlpra2 and rcd1 mutant retinas again support enhanced NO production levels as a component of the disease process.

IHC analysis of NOS2 (iNOS) in normal and mutant retinas confirmed the localization of NOS2 to the GCL in normal retinas at the three time points examined (Figure 6a A–C). The mutants also showed immunolabeling in the GCL but with greater intensity than controls (Figure 6). As with NOS1, the xlpra2 and rcd1 retinas showed more intense and diffuse labeling in the nuclear and plexiform layers (Figure 6a E, H, I); additionally, the inner segments of the 12–16 weeks xlpra2 retina showed enhanced labeling in the remaining inner segments (Figure 6a E). Finally, results of qRT-PCR analysis on retina samples showed increased levels of NOS2 mRNA expression in retinas from crd2 groups compared to retinas from normal dogs (Figure 6b), further supporting the potential for increased NO generation in affected animals. We were unable to show iNOS protein expression because of

unsuccessful western blot analysis. The source of antibody used for IHC and western blot experiments is mentioned in Table 3.

**Increased levels of 4HNE in retinal degeneration—**Peroxidation of PUFAs within the cell membrane of photoreceptors results in the production of the toxic metabolite 4HNE (Dalleau et al., 2013). This occurs downstream of NO production and generation of ROS (Figure 1, Pathway 3). To determine if 4HNE is produced in photoreceptors, cryosections of retinas from different age groups were labeled with an antibody against 4HNE. IHC showed an age-related increase in 4HNE localization at the membrane of photoreceptors in the affected dogs. In normal retinas, labeling changed from the outer segment at the age of five weeks to the inner segment at later time points (Figure 7a and b). Specifically, the intensity of signals was higher in the mutant photoreceptors at 12–16 weeks compared to normal (Figure 7b B, E, H, K). IHC also showed that the intensity of 4HNE signals increased with aging in xlpra2 and rcd1 retinas at the older time points, but not in crd2 (Figure 7b F, I, L), likely the result of disease-associated photoreceptor loss in the latter disease.

Western blot analysis was then performed to assay for the presence of 4HNE in the retinas of normal and diseased animals (Figure 7c). Densitometry analysis showed a significantly higher level of 4HNE in xlpra2 and rcd1 retinas, with levels 2.55 and 2.53-fold higher than in the normal retina, respectively (one-way ANOVA, $p<0.01$). Although 4HNE levels also were increased in crd2, these were not statistically significant (Figure 7d). As indicated above, increased levels of 4HNE in xlpra2 and rcd1 retinas suggest a high level of lipid peroxidation and oxidative damage in these two models.

**Levels of acrolein increase in affected retinas—**Acrolein is another toxic metabolite of lipid peroxidation (Figure 1, Pathway 3). To examine the localization of this molecule, retinal cryosections were labeled with an antibody against acrolein. In normal retinas, acrolein was mainly present in the GCL (Figure 8). At 5 weeks of age, there were no immunolabeling differences between the normal and mutant retinas (Figure 8 D, G, J). However, at the older time points, particularly 12–16 weeks when active degeneration was ongoing, the intensity of the acrolein labeling increased in PR, INL, and GCL in retinas of mutants Figure 8 E, H, K). We could not show increased levels of acrolein by western blot. The source of antibody used for IHC and western blot experiments is mentioned in Table 3.

**BCL2 expression in retinal degenerative diseases—**BCL2 is an anti-apoptotic protein in the mitochondrial membrane, and its reduced expression results in the initiation of apoptosis. Quantitative PCR analysis of retina samples revealed increased levels of BCL2 mRNA expression in rcd1 retinas, but levels remained unchanged in crd2 and were elevated but not significantly in xlpra2 (Figure 9a). However, western blot analysis (Figure 9b) revealed a lower level of BCL2 protein in the three retinal disease models, and these were statistically significant for xlpra2 and crd2 (one-way ANOVA, $p<0.01$) (Figure 9b, c). Decreased BcL2 expression in these retinas at an early age suggests that apoptosis initiation in these diseases is associated with the intrinsic mitochondrial cell death pathway.

## Discussion

This study evaluated gene, and protein expression levels of TSP enzymes, NO producing enzymes, BCL2, and as well as lipid metabolites levels as a marker for oxidative damage, in retinas of dogs having 3 non-allelic, early-onset inherited retinal degenerations (Gardiner et al., 2016; Goldstein et al., 2013). These proteins are key players in the TSP and redox homeostasis interactome. Although we could not measure $H_2S$ or NO directly, we analyzed the specific proteins involved in their production and downstream effectors.

CBS and CSE, the key enzymes of TSP, are responsible for $H_2S$ and GSH production. Previously we showed that CBS and CSE are expressed in canine, human and non-human primate (NHP) retinas (Badiei et al., 2019). We now report that qRT-PCR results showed increased CBS mRNA levels in mutant retinas, and western analyses confirmed significant increases of CBS in rcd1 and crd2 retinas, but not xlpra2. RNA-Seq data analyses of xlpra2 and rcd1 retinas published independently by our research group showed increased RNA levels of CBS but not CSE (Sudharsan et al., 2017) in xlpra2 and rcd1 affected canine retinas, and the current findings are consistent with this report. IHC results also showed an increased intensity of CBS protein expression, mainly in the GCL of affected dogs compared to normal.

CBS is one of the main enzymes that contribute to endogenous $H_2S$ production in the retina, and its overexpression can result in increased levels of $H_2S$. The higher concentration of $H_2S$ is toxic and may contribute to the pathogenesis of retinal degeneration in mutant retinas. Although $H_2S$ plays a protective role at physiological levels, it has cytotoxic impacts at higher concentrations via inhibition of mitochondrial cytochrome C oxidase, DNA damage, and pro-inflammatory effects (Han et al., 2019). $H_2S$ also contributes to ROS formation in a concentration-dependent manner. H2S plays a neuroprotective role in lower concentrations by preventing ROS generation and accumulation of lipid peroxidation products, while in high concentrations, $H_2S$ causes ROS formation (Shefa et al., 2018). The increased levels of CBS in this study can result in the generation of toxic levels of $H_2S$, suggesting that the defense systems against constitutive oxidative stress are not compatible. Increased levels of $H_2S$ may also contribute to retinal degeneration via its role in apoptosis. It protects against light-induced photoreceptor apoptosis by regulating $Ca^{+2}$ homeostasis (Mikami et al., 2011) but in its toxic levels, might exacerbate the progression of retinal degeneration by increasing the cyclic nucleotide, adenosine 3′,5′ cyclic monophosphate (cAMP) concentration in RPE cells dose-dependently (Njie-Mbye et al., 2010). Increased cAMP levels can be toxic and cause retina cell death and progression of retinal degenerative disease (Hall et al., 1993; Traverso et al., 2002). Intracellular cyclic guanosine monophosphate (cGMP) can influence the intracellular concentration of cAMP (Zaccolo and Movsesian, 2007). cAMP increases NO through activation of protein kinase A (Zhang and Hintze, 2001) and NO increase cGMP levels while cGMP in return reduces the cAMP signals through phosphodiesterases (Polito et al., 2013). $H_2S$ reduces cGMP levels and prevents NO-induced increase in cGMP (Salomone et al, 2014). This activity of $H_2S$ might be related to its inhibitory effect on NO production (Badiei et al., 2013).

Western blot results showed increased levels of nNOS protein in the retinas of xlpra2 and rcd1 affected dogs. qRT-PCR results also showed increased NOS2 (iNOS) gene expression levels in affected dogs aged 12–16 weeks. IHC results also confirmed increased iNOS immunolabeling in affected retinas at the age of 12–16 weeks. iNOS-derived NO contributes to neurodegeneration, diabetic retinopathy, and cell apoptosis, and NO overproduced by nNOS is toxic for RGCs and mediates retina injury (Opatrilova et al., 2018; Mishra and Newman, 2010; Sennlaub et al., 2002). As NO produced by iNOS can damage mitochondria (Li et al., 2005; Snyder et al., 2009) and contribute to the apoptosis and sustained damage to retina cells, the increased iNOS expression in affected retinas might play a role in retina cell death. nNOS mediates light-induced photoreceptor apoptosis, and inhibition of nNOS activity reduces photoreceptor apoptosis and retinal degeneration (Donovan et al., 2001). Overproduced NO regulates BCL2 expression to trigger cell death (Snyder et al., 2009). While qPCR results showed increased levels of BCL2 mRNA in rcd1 mutant dogs but not in crd2 nor in xlpra2, there was a decrease of BCL2 protein levels in all three models in the 7.7–11.7-week time period. This age is immediately after the peak of cell death, at a time when there are markedly elevated numbers of TUNEL positive cells (Genini et al.,2013; Downs et al., 2016). The decrease in BCL2 protein suggests that increased permeability of mitochondria membranes leads to mitochondrial dysfunction in these diseases. BCL2 plays a key role in cell survival, and overexpression of this protein prevents neuronal cell death by decreasing the ROS generation (Kane et al., 1993) and increasing GSH levels (Voehringer and Meyn, 2000). GSH homeostasis is related to BCL2 expression in the retina (Park et al., 2013), and decreased BCL2 levels in diseased retinas in this study can affect GSH redox status.

Lipid damage and peroxidation play a key role in retinal cell death. Chronic light exposure also promotes intense lipid peroxidation in the retina (Wiegand et al., 1983; Organisciak et al., 1992) and induces death of photoreceptors cells via apoptosis (Hafezi et al., 1997). 4HNE, a toxic product of peroxidation of PUFAs, is considered an important marker of oxidative stress that drives the pathology of retinal diseases (Tanito et al., 2005; Shoeb et al., 2014). Western blot results showed increases in 4HNE production in the 3 models, and the elevation was significant in xlpra2 and rcd1. Immunohistochemistry confirmed high 4HNE immunofluorescence in photoreceptor cells at the 12–16 weeks time point, but not earlier. As high concentrations of 4HNE play a key role in inducing apoptosis (Cheng et al., 2001; Yang et al., 2003), the increased levels of 4HNE in our study suggest that oxidative stress and associated damage contribute to degeneration in mutant retinas.

Acrolein is another toxic product of lipid peroxidation that increases oxidative stress, depletes GSH, and causes mitochondrial damages (Alfarhan et al., 2020). We also found the increased intensity of acrolein immunolabeling in diseased retinas at the same time period, 12–16 weeks, a possible indication that reduced levels of GSH and mitochondrial dysfunction were occurring. This is consistent with previous in vitro studies showing that acrolein treatment reduces GSH levels in RPE and Müller cells and damages mitochondria (Murata et al., 2019; Feng et al., 2010). Both acrolein and 4HNE are detoxified in conjunction with GSH (Zhang et al., 2010; Engle et al., 2004; Srivastava et al., 1998), resulting in depletion of GSH (Feng et al., 2010; Jia et al., 2007), and the reduction of this defense mechanism to protect against additional oxidative stress.

In conclusion, our findings provide evidence that the upregulation of CBS, but not CSE, in retinal degenerative diseases indicates a potential increase in levels of $H_2S$ and contribute to the disease process. $H_2S$ exerts pharmacological effects on neuronal tissues and can play a neuroprotective role in the retina through scavenging toxic products, anti-apoptotic, antioxidant activity, and regulation of NO levels when present at low levels. However, high levels of $H_2S$ in affected retinas can result in enhanced levels of ROS. Excessive NO production due to increased nNOS and iNOS expression affects mitochondrial function by reducing BCL2 and triggering apoptosis. Increased levels of 4HNE and acrolein, markers for oxidative stress, also confirm ongoing lipid peroxidation of retinal cell membranes, primarily photoreceptor outer segments. Further studies would inform our understanding of the specific role of $H_2S$ in retinal degenerations and the mechanism by which $H_2S$ induces these effects.

## Acknowledgment

The authors thank RDS facility staff for their assistance in providing archived retinal samples used in this study. We are also grateful to Dr. Leslie King and Peter K Cooper for editorial advice and helpful suggestions and Lydia Melnyk for research coordination. This research is supported by an NEI/NIH EY-06855 and -17549, Foundation Fighting Blindness (FFB), Van Sloun Fund for Canine Genetic Research.

## References

Aguirre GD 2017. ‘Concepts and Strategies in Retinal Gene Therapy,’ Invest Ophthalmol Vis Sci. 58, 5399–411. [PubMed: 29053763]

Alfarhan M, Jafari E, and Narayanan SP. 2020. ‘Acrolein: A Potential Mediator of Oxidative Damage in Diabetic Retinopathy,’ Biomolecules. 10.

Ao J, Wood JP, Chidlow G, Gillies MC, Casson RJ 2018 ‘Retinal pigment epithelium in the pathogenesis of age-related macular degeneration and photobiomodulation as a potential therapy?’ Clin Exp Ophthalmol. 46(6): p. 670–686. [PubMed: 29205705]

Badiei A, Chambers ST, Gaddam RR, and Bhatia M. 2016. ‘Cystathionine-gamma-lyase gene silencing with siRNA in monocytes/ macrophages attenuates inflammation in cecal ligation and puncture-induced sepsis in the mouse,’ J Biosci. 41, 87–95. [PubMed: 26949091]

Badiei A, Rivers-Auty J, Ang AD, and Bhatia M. 2013. ‘Inhibition of hydrogen sulfide production by gene silencing attenuates inflammatory activity of LPS-activated RAW264.7 cells’, Appl Microbiol Biotechnol. 97, 7845–52. [PubMed: 23838794]

Badiei A, Sudharsan R, Santana E, Dunaief JL, and Aguirre GD. 2019. ‘Comparative localization of cystathionine beta synthases and cystathionine gamma-lyase in canine, non-human primate, and human retina,’ Exp Eye Res. 181, 72–84. [PubMed: 30653965]

Bhatia M 2012. ‘Role of hydrogen sulfide in the pathology of inflammation, Scientifica (Cairo), 2012, 159680. [PubMed: 24278674]

Brown GC 1992. ‘Control of respiration and ATP synthesis in mammalian mitochondria and cells,’ Biochem J. 284 ( Pt 1), 1–13. [PubMed: 1599389]

Cheng JZ, Singhal SS, Sharma A, Saini M, Yang Y, Awasthi S, Zimniak P, and Awasthi YC. 2001. ‘Transfection of mGSTA4 in HL-60 cells protects against 4-hydroxynonenal-induced apoptosis by inhibiting JNK-mediated signaling’, Arch Biochem Biophys. 392, 197–207. [PubMed: 11488593]

Dalleau S, Baradat M, Gueraud F, and Huc L. 2013. ‘Cell death and diseases related to oxidative stress: 4-hydroxynonenal (HNE) in the balance’, Cell Death Differ. 20, 1615–30. [PubMed: 24096871]

Donovan M, Carmody RJ, and Cotter TG. 2001. ‘Light-induced photoreceptor apoptosis in vivo requires neuronal nitric-oxide synthase and guanylate cyclase activity and is caspase-3-independent’, J Biol Chem. 276, 23000–8. [PubMed: 11278285]

Downs LM, Scott EM, Cideciyan AV, Iwabe S, Dufour V, Gardiner KL, Genini S, Marinho LF, Sumaroka A, Koszyk MS, Swider M, Aguirre GK, Jacobson SG, Beltran WA, and Aguirre GD. 2016. 'Overlap of abnormal photoreceptor development and progressive degeneration in Leber congenital amaurosis caused by NPHP5 mutation', Hum Mol Genet. 25, 4211–26. [PubMed: 27506978]

Du J, Jin H, and Yang L. 2017. 'Role of Hydrogen Sulfide in Retinal Diseases,' Front Pharmacol, 8: 588. [PubMed: 28900398]

Engle MR, Singh SP, Czernik PJ, Gaddy D, Montague DC, Ceci JD, Yang Y, Awasthi S, Awasthi YC, and Zimniak P. 2004. 'Physiological role of mGSTA4–4, a glutathione S-transferase metabolizing 4-hydroxynonenal: generation and analysis of mGsta4 null mouse', Toxicol Appl Pharmacol. 194, 296–308. [PubMed: 14761685]

Erisgin Z, Ozer MA, Tosun M, Ozen S, and Takir S. 2019. 'The effects of intravitreal H2 S application on apoptosis in the retina and cornea in experimental glaucoma model', Int J Exp Pathol. 100, 330–36. [PubMed: 31777145]

Feng Z, Liu Z, Li X, Jia H, Sun L, Tian C, Jia L, and Liu J. 2010. 'alpha-Tocopherol is an effective Phase II enzyme inducer: protective effects on acrolein-induced oxidative stress and mitochondrial dysfunction in human retinal pigment epithelial cells,' J Nutr Biochem. 21, 1222–31. [PubMed: 20153624]

Finkelstein JD 1990. 'Methionine metabolism in mammals,' J Nutr Biochem.1, 228. [PubMed: 15539209]

Fliesler SJ, and Anderson RE. 1983. 'Chemistry and metabolism of lipids in the vertebrate retina,' Prog Lipid Res. 22, 79–131. [PubMed: 6348799]

Fuhrmann S, Zou C, and Levine EM, Retinal pigment epithelium development, plasticity, and tissue homeostasis. Exp Eye Res, 2014. 123: p. 141–50. [PubMed: 24060344]

Ganea E, and Harding JJ. 2006. 'Glutathione-related enzymes and the eye,' Curr Eye Res, 31: 1–11. [PubMed: 16421014]

Gardiner KL, Downs L, Berta-Antalics AI, Santana E, Aguirre GD, and Genini S. 2016. 'Photoreceptor proliferation and dysregulation of cell cycle genes in early-onset inherited retinal degenerations,' BMC Genomics. 17, 221. [PubMed: 26969498]

Genini S, Beltran WA, and Aguirre GD. 2013. 'Up-regulation of tumor necrosis factor superfamily genes in early phases of photoreceptor degeneration,' PLoS One. 8, e85408. [PubMed: 24367709]

Goldstein O, Mezey JG, Schweitzer PA, Boyko AR, Gao C, Bustamante CD, Jordan JA, Aguirre GD, and Acland GM. 2013. 'IQCB1 and PDE6B mutations cause similar early onset retinal degenerations in two closely related terrier dog breeds', Invest Ophthalmol Vis Sci. 54, 7005–19. [PubMed: 24045995]

Hafezi F, Steinbach JP, Marti A, Munz K, Wang ZQ, Wagner EF, Aguzzi A, and Reme CE. 1997. 'The absence of c-fos prevents light-induced apoptotic cell death of photoreceptors in retinal degeneration in vivo,' Nat Med. 3, 346–9. [PubMed: 9055866]

Hall MO, Abrams TA, and Mittag TW. 1993. 'The phagocytosis of rod outer segments is inhibited by drugs linked to cyclic adenosine monophosphate production,' Invest Ophthalmol Vis Sci. 34, 2392–401. [PubMed: 7686891]

Han Y, Shang Q, Yao J, and Ji Y. 2019. 'Hydrogen sulfide: a gaseous signaling molecule modulates tissue homeostasis: implications in ophthalmic diseases,' Cell Death Dis. 10, 293. [PubMed: 30926772]

Haq E, Rohrer B, Nath N, Crosson CE, and Singh I. 2007. 'S-nitrosoglutathione prevents interphotoreceptor retinoid-binding protein (IRBP(161–180))-induced experimental autoimmune uveitis', J Ocul Pharmacol Ther. 23, 221–31. [PubMed: 17593005]

Jarrett SG, Lin H, Godley BF, and Boulton ME. 2008. 'Mitochondrial DNA damage and its potential role in retinal degeneration,' Prog Retin Eye Res. 27, 596–607. [PubMed: 18848639]

Jia L, Liu Z, Sun L, Miller SS, Ames BN, Cotman CW, and Liu J. 2007. 'Acrolein, a toxicant in cigarette smoke, causes oxidative damage and mitochondrial dysfunction in RPE cells: protection by (R)-alpha-lipoic acid,' Invest Ophthalmol Vis Sci. 48, 339–48. [PubMed: 17197552]

Kane DJ, Sarafian TA, Anton R, Hahn H, Gralla EB, Valentine JS, Ord T, and Bredesen DE. 1993. 'Bcl-2 inhibition of neural death: decreased generation of reactive oxygen species', Science. 262, 1274–7. [PubMed: 8235659]

Li J, Baud O, Vartanian T, Volpe JJ, and Rosenberg PA. 2005. 'Peroxynitrite generated by inducible nitric oxide synthase and NADPH oxidase mediates microglial toxicity to oligodendrocytes', Proc Natl Acad Sci U S A. 102, 9936–41. [PubMed: 15998743]

Liang FQ, Alssadi R, Morehead P, Awasthi YC, and Godley BF. 2005. 'Enhanced expression of glutathione-S-transferase A1–1 protects against oxidative stress in human retinal pigment epithelial cells', Exp Eye Res. 80, 113–9. [PubMed: 15652532]

Locksley RM, Killeen N, and Lenardo MJ. 2001. 'The TNF and TNF receptor superfamilies: integrating mammalian biology,' Cell. 104, 487–501. [PubMed: 11239407]

Mikami Y, Shibuya N, Kimura Y, Nagahara N, Yamada M, and Kimura H. 2011. 'Hydrogen sulfide protects the retina from light-induced degeneration by the modulation of Ca2+ influx', J Biol Chem. 286, 39379–86. [PubMed: 21937432]

Mishra A, and Newman EA. 2010. 'Inhibition of inducible nitric oxide synthase reverses the loss of functional hyperemia in diabetic retinopathy,' Glia. 58, 1996–2004. [PubMed: 20830810]

Murata M, Noda K, Yoshida S, Saito M, Fujiya A, Kanda A, and Ishida S. 2019. 'Unsaturated Aldehyde Acrolein Promotes Retinal Glial Cell Migration,' Invest Ophthalmol Vis Sci. 60, 4425–35. [PubMed: 31652327]

Njie-Mbye YF, Bongmba OY, Onyema CC, Chitnis A, Kulkarni M, Opere CA, LeDay AM, and Ohia SE. 2010. 'Effect of hydrogen sulfide on cyclic AMP production in isolated bovine and porcine neural retinae,' Neurochem Res. 35, 487–94. [PubMed: 19898983]

Opatrilova R, Kubatka P, Caprnda M, Busselberg D, Krasnik V, Vesely P, Saxena S, Ruia S, Mozos I, Rodrigo L, Kruzliak P, and Dos Santos KG. 2018. 'Nitric oxide in the pathophysiology of retinopathy: evidences from preclinical and clinical researches,' Acta Ophthalmol. 96, 222–31. [PubMed: 28391624]

Organisciak DT, Darrow RM, Jiang YI, Marak GE, and Blanks JC. 1992. 'Protection by dimethylthiourea against retinal light damage in rats', Invest Ophthalmol Vis Sci. 33, 1599–609. [PubMed: 1559759]

Park MH, Kim SY, Moon C, Bae YC, Moon JI, and Moon C. 2013. 'Differential cell death and Bcl-2 expression in the mouse retina after glutathione decrease by systemic D,L-buthionine sulphoximine administration', Mol Cells. 35, 235–42. [PubMed: 23430084]

Parsanathan R and Jain SK. 2018. 'Hydrogen sulfide increases glutathione biosynthesis, and glucose uptake and utilisation in C2C12 mouse myotubes,' Free Radic Res. 52, 288–303. [PubMed: 29378451]

Polito M, Klarenbeek J, Jalink K, Paupardin-Tritsch D, Vincent P, Castro LR 2013.'The NO/cGMP pathway inhibits transient cAMP signals through the activation of PDE2 in striatal neurons,' Front Cell Neurosci. 7, 211. [PubMed: 24302895]

Portera-Cailliau C, Sung CH, Nathans J, and Adler R. 1994. 'Apoptotic photoreceptor cell death in mouse models of retinitis pigmentosa,' Proc Natl Acad Sci U S A. 91, 974–8. [PubMed: 8302876]

Rajala RV, and Rajala A. 2013. 'Neuroprotective role of protein tyrosine phosphatase-1B in rod photoreceptor neurons', Protein Cell. 4, 890–2. [PubMed: 24203758]

Ray K, Baldwin VJ, Acland GM, Blanton SH, and Aguirre GD. 1994. 'Cosegregation of codon 807 mutation of the canine rod cGMP phosphodiesterase beta gene and rcd1', Invest Ophthalmol Vis Sci. 35, 4291–9. [PubMed: 8002249]

Roh YJ, Moon C, Kim SY, Park MH, Bae YC, Chun MH, and Moon JI. 2007. 'Glutathione depletion induces differential apoptosis in cells of mouse retina, in vivo,' Neurosci Lett. 417, 266–70. [PubMed: 17400377]

Salomone S, Foresti R, Villari A, Giurdanella G, Drago F, Bucolo C 2014. 'Regulation of vascular tone in rabbit ophthalmic artery: cross talk of endogenous and exogenous gas mediators,' Biochem Pharmacol. 92, 661–8. [PubMed: 25451691]

Sennlaub F, Courtois Y, and Goureau O. 2002. 'Inducible nitric oxide synthase mediates retinal apoptosis in ischemic proliferative retinopathy,' J Neurosci. 22, 3987–93. [PubMed: 12019318]

Sharma A, Sharma R, Chaudhary P, Vatsyayan R, Pearce V, Jeyabal PV, Zimniak P, Awasthi S, and Awasthi YC. 2008. '4-Hydroxynonenal induces p53-mediated apoptosis in retinal pigment epithelial cells', Arch Biochem Biophys. 480, 85–94. [PubMed: 18930016]

Shefa U, Kim MS, Jeong NY, and Jung J. 2018. 'Antioxidant and Cell-Signaling Functions of Hydrogen Sulfide in the Central Nervous System,' Oxid Med Cell Longev. 2018: 1873962. [PubMed: 29507650]

Shoeb M, Ansari NH, Srivastava SK, and Ramana KV. 2014. '4-Hydroxynonenal in the pathogenesis and progression of human diseases', Curr Med Chem. 21, 230–7. [PubMed: 23848536]

Singh S, Padovani D, Leslie RA, Chiku T, and Banerjee R. 2009. 'Relative contributions of cystathionine beta-synthase and gamma-cystathionase to H2S biogenesis via alternative transsulfuration reactions', J Biol Chem. 284, 22457–66. [PubMed: 19531479]

Siu AW, Shan SW, Li KK, Lam HY, Fung MY, Li KK, To CH, and Do CW. 2015. 'Glutathione attenuates nitric oxide-induced retinal lipid and protein changes,' Ophthalmic Physiol Opt. 35, 135–46. [PubMed: 25761579]

Siu AW, and To CH. 2002. 'Nitric oxide and hydroxyl radical-induced retinal lipid peroxidation in vitro,' Clin Exp Optom. 85, 378–82. [PubMed: 12452789]

Snyder CM, Shroff EH, Liu J, and Chandel NS. 2009. 'Nitric oxide induces cell death by regulating anti-apoptotic BCL-2 family members', PLoS One. 4, e7059. [PubMed: 19768117]

Srivastava S, Chandra A, Wang LF, Seifert WE Jr., DaGue BB, Ansari NH, Srivastava SK, and Bhatnagar A. 1998. 'Metabolism of the lipid peroxidation product, 4-hydroxy-trans-2-nonenal, in isolated perfused rat heart', J Biol Chem. 273, 10893–900. [PubMed: 9556565]

Stipanuk MH 2004. 'Sulfur amino acid metabolism: pathways for production and removal of homocysteine and cysteine,' Annu Rev Nutr. 24, 539–77. [PubMed: 15189131]

Sudharsan R, Beiting DP, Aguirre GD, and Beltran WA. 2017. 'Involvement of Innate Immune System in Late Stages of Inherited Photoreceptor Degeneration,' Sci Rep. 7, 17897. [PubMed: 29263354]

Szabo C, Ransy C, Modis K, Andriamihaja M, Murghes B, Coletta C, Olah G, Yanagi K, and Bouillaud F. 2014. 'Regulation of mitochondrial bioenergetic function by hydrogen sulfide. Part I. Biochemical and physiological mechanisms', Br J Pharmacol. 171, 2099–122. [PubMed: 23991830]

Tanito M, Elliott MH, Kotake Y, and Anderson RE. 2005. 'Protein modifications by 4-hydroxynonenal and 4-hydroxyhexenal in light-exposed rat retina', Invest Ophthalmol Vis Sci. 46, 3859–68. [PubMed: 16186375]

Traverso V, Bush RA, Sieving PA, and Deretic D. 2002. 'Retinal cAMP levels during the progression of retinal degeneration in rhodopsin P23H and S334ter transgenic rats', Invest Ophthalmol Vis Sci. 43, 1655–61. [PubMed: 11980887]

Voehringer DW, and Meyn RE. 2000. 'Redox aspects of Bcl-2 function', Antioxid Redox Signal. 2, 537–50. [PubMed: 11229367]

Wang C, and Youle RJ. 2009. 'The role of mitochondria in apoptosis*,' Annu Rev Genet, 43: 95–118. [PubMed: 19659442]

Wenzel A, Grimm C, Samardzija M, and Reme CE. 2005. 'Molecular mechanisms of light-induced photoreceptor apoptosis and neuroprotection for retinal degeneration,' Prog Retin Eye Res. 24, 275–306. [PubMed: 15610977]

Wiegand RD, Giusto NM, Rapp LM, and Anderson RE. 1983. 'Evidence for rod outer segment lipid peroxidation following constant illumination of the rat retina,' Invest Ophthalmol Vis Sci. 24, 1433–5. [PubMed: 6618806]

Yang Y, Sharma A, Sharma R, Patrick B, Singhal SS, Zimniak P, Awasthi S, and Awasthi YC. 2003. 'Cells preconditioned with mild, transient UVA irradiation acquire resistance to oxidative stress and UVA-induced apoptosis: role of 4-hydroxynonenal in UVA-mediated signaling for apoptosis', J Biol Chem. 278, 41380–8. [PubMed: 12888579]

Zaccolo M and Movsesian MA. 2007. 'cAMP and cGMP signaling cross-talk: role of phosphodiesterases and implications for cardiac pathophysiology,' Circ Res. 100, 1569–78. [PubMed: 17556670]

Zhang M, Shoeb M, Goswamy J, Liu P, Xiao TL, Hogan D, Campbell GA, and Ansari NH. 2010. 'Overexpression of aldehyde dehydrogenase 1A1 reduces oxidation-induced toxicity in SH-SY5Y neuroblastoma cells', J Neurosci Res. 88, 686–94. [PubMed: 19774675]

Zhang Q, Acland GM, Wu WX, Johnson JL, Pearce-Kelling S, Tulloch B, Vervoort R, Wright AF, and Aguirre GD. 2002. 'Different RPGR exon ORF15 mutations in Canids provide insights into photoreceptor cell degeneration', Hum Mol Genet. 11, 993–1003. [PubMed: 11978759]

Zhang X and Hintze TH. 2015. 'cAMP signal transduction cascade, a novel pathway for the regulation of endothelial nitric oxide production in coronary blood vessels,' Arterioscler Thromb Vasc Biol. 21, 797–803.

- Alterations in the expression of enzymes directly involved in maintaining the normal redox status of the retina during retinal degeneration.
- Increased levels of cystathionine β–synthase (CBS), an enzyme that produces $H_2S$ in neurons, in retinal degeneration, but not those of cystathionine γ-lyase (CSE), an enzyme involved in production of glutathione (GSH), an antioxidant.
- Increased levels of $H_2S$ that are not counterbalanced by increased antioxidant potential may contribute to disease in affected retinas.
- Decreased levels of BCL2, an anti-apoptotic protein in the mitochondrial membrane in affected retinas with increased levels of toxic products such as acrolein and hydroxynonenal (4HNE), together with increased levels of NO, $H_2S$, and ROS likely render photoreceptors susceptible to an intrinsic apoptotic pathway involving mitochondrial membranes.

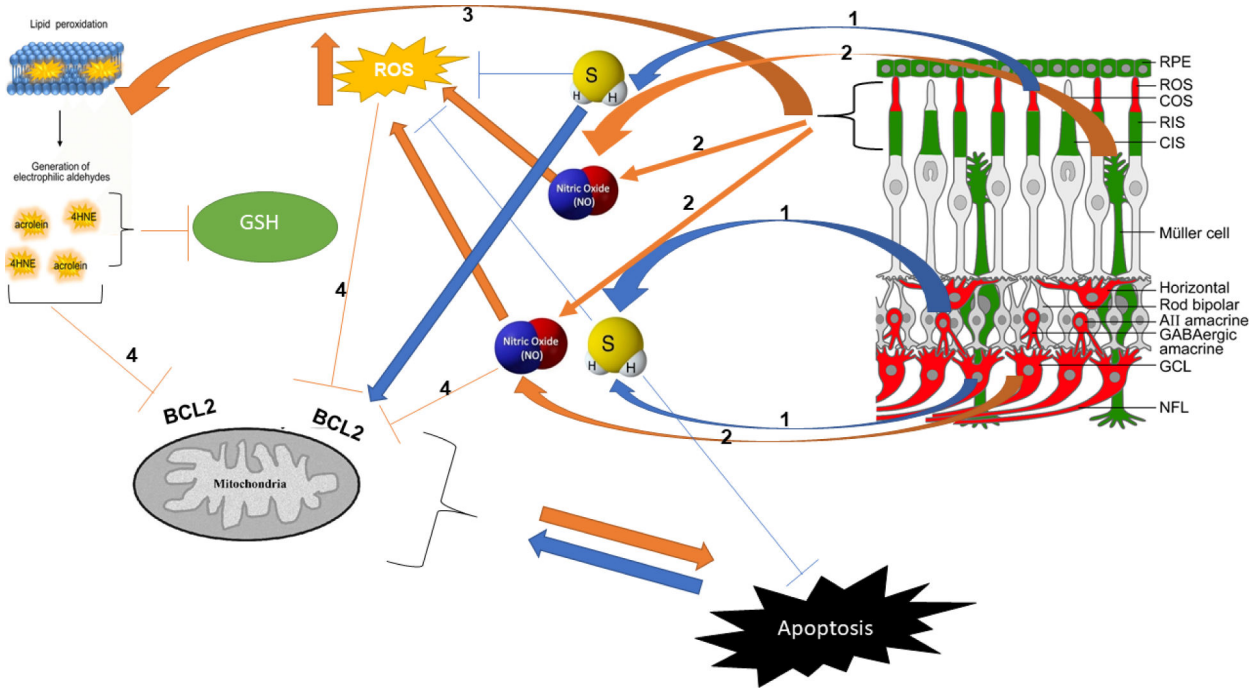


**Figure 1.**

Lipid peroxidation, NO, and molecules produced by TSP enzymes affect the apoptosis pathway in retinal degenerative diseases. Schematic representation of $H_2S$ and NO molecules produced in retina and interaction with ROS products. Key molecules and components of the pathway: (1) CBS and CSE are the main enzymes of TSP involved in $H_2S$ and GSH production in the retina. Physiological level of $H_2S$ is shown to have neuroprotective effects. (2) NO is a gaseous molecule that affects BCL2 and mitochondrial function, and excessive NO produced in retinal degeneration is detrimental to retinal cells. (3) The photoreceptor membrane is rich in PUFA and is vulnerable to peroxidation because of chronic light exposure. High metabolic rate and high levels of oxygen levels result in ROS production. Increased levels of ROS lead to the peroxidation of PUFAs. (4) Acrolein and 4HNE are the metabolites of PUFAs peroxidation that, along with ROS, can affect GSH and BCL2 and cause mitochondrial dysfunction. The schematic of the retina on the top right was modified from Figure 9 of Badiei et al. Exp. Eye. Res. (2019) and shows immunolocalization of CBS (red) and CSE (green) in retinal neurons and subcellular compartments.

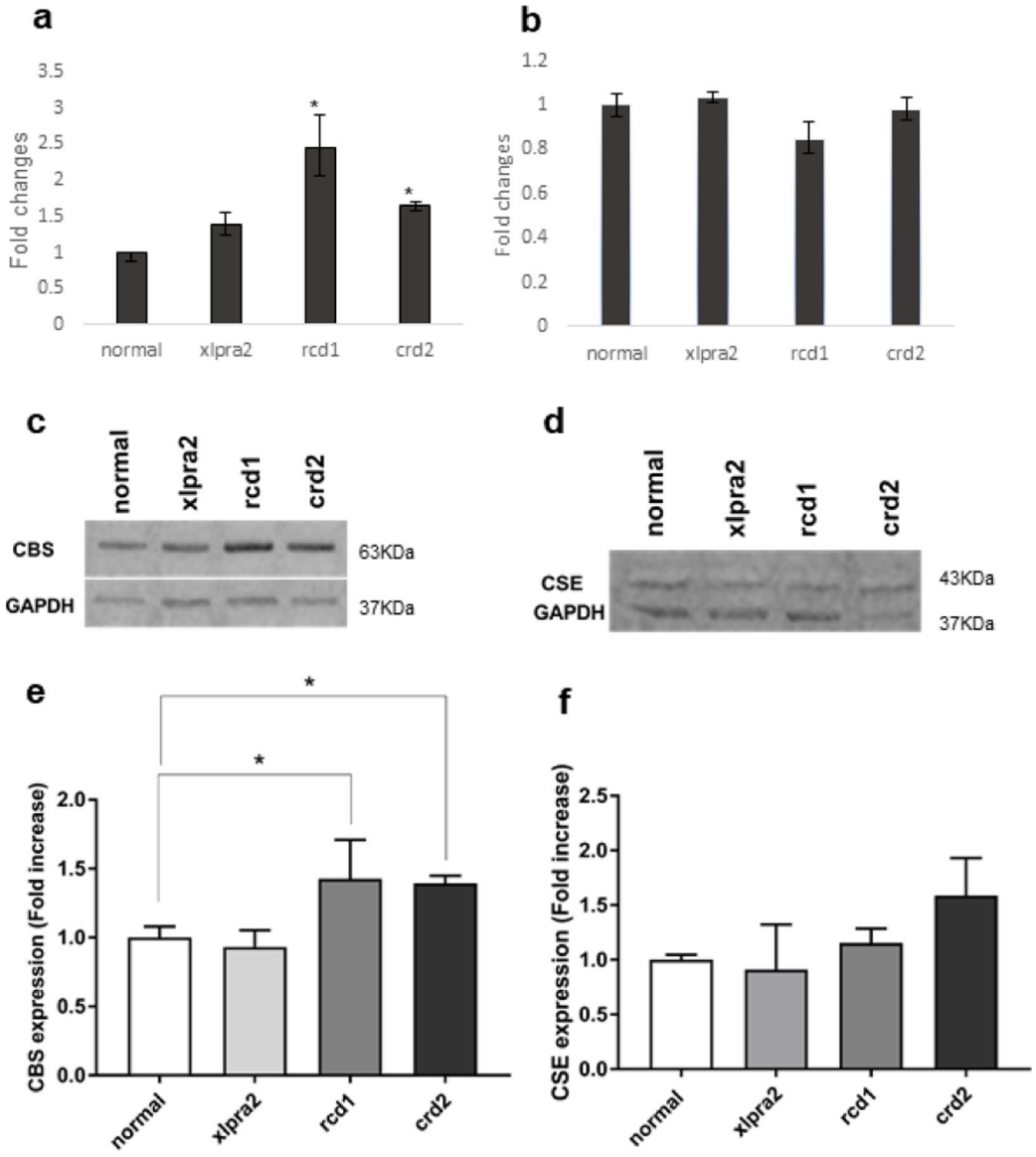


**Figure 2.**

qRT-PCR, western blot, densitometry analysis of CBS and CSE gene and protein expression in normal canine control and, xlpra2, rcd1 and crd2 diseases taken in 7.7–13.6 weeks of age time window (see Table 1). CBS (a) and CSE (b) mRNA expression was normalized with GAPDH gene and expressed as fold change. The results showed an increase in CBS but not CSE expression in the 3 retinal disease models; CBS increase was significant in rcd1 and crd2. CBS protein levels in the rcd1 and crd2 groups were significantly higher than normal samples (c and e). CSE protein levels did not change in affected dogs compared to normal dogs (d and f). The results are shown as the means ± SD. The significance of difference among groups was evaluated by a one-way ANOVA with a post hoc 'Tukey's test. (One-way ANOVA, *P < 0.05).

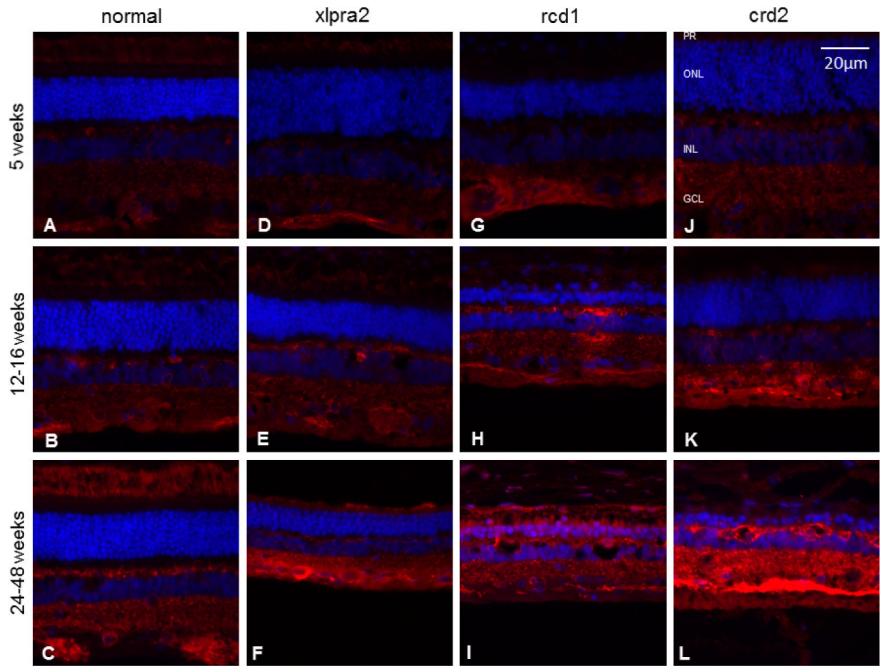


**Figure 3.**

Immunohistochemistry of CBS (red fluorescence) in normal and mutant retinas of different ages. With the progression of the disease, immunolabeling intensity increases in the GCL. Labeling of the inner and outer plexiform layers also increases in the older rcd1 and crd2 mutant retinas. DAPI (blue) nuclear stain. Scale bar: 20 µm; PR: Photoreceptor cells, ONL: outer nuclear layer; INL: inner nuclear layer; GCL: ganglion cell layer.

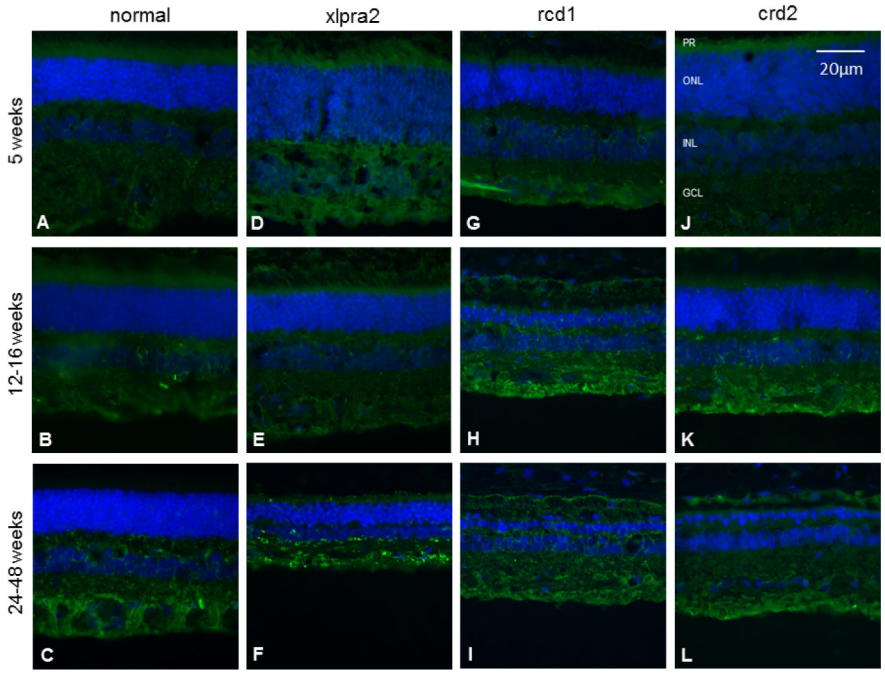


**Figure 4.**

Immunohistochemical analysis of CSE (green fluorescence) of normal and mutant retinas of different ages. There is little change in CSE expression with age or disease. DAPI (blue) nuclear stain. Scale bar: 20 µm; PR: Photoreceptor cells, ONL: outer nuclear layer; INL: inner nuclear layer; GCL: ganglion cell layer.

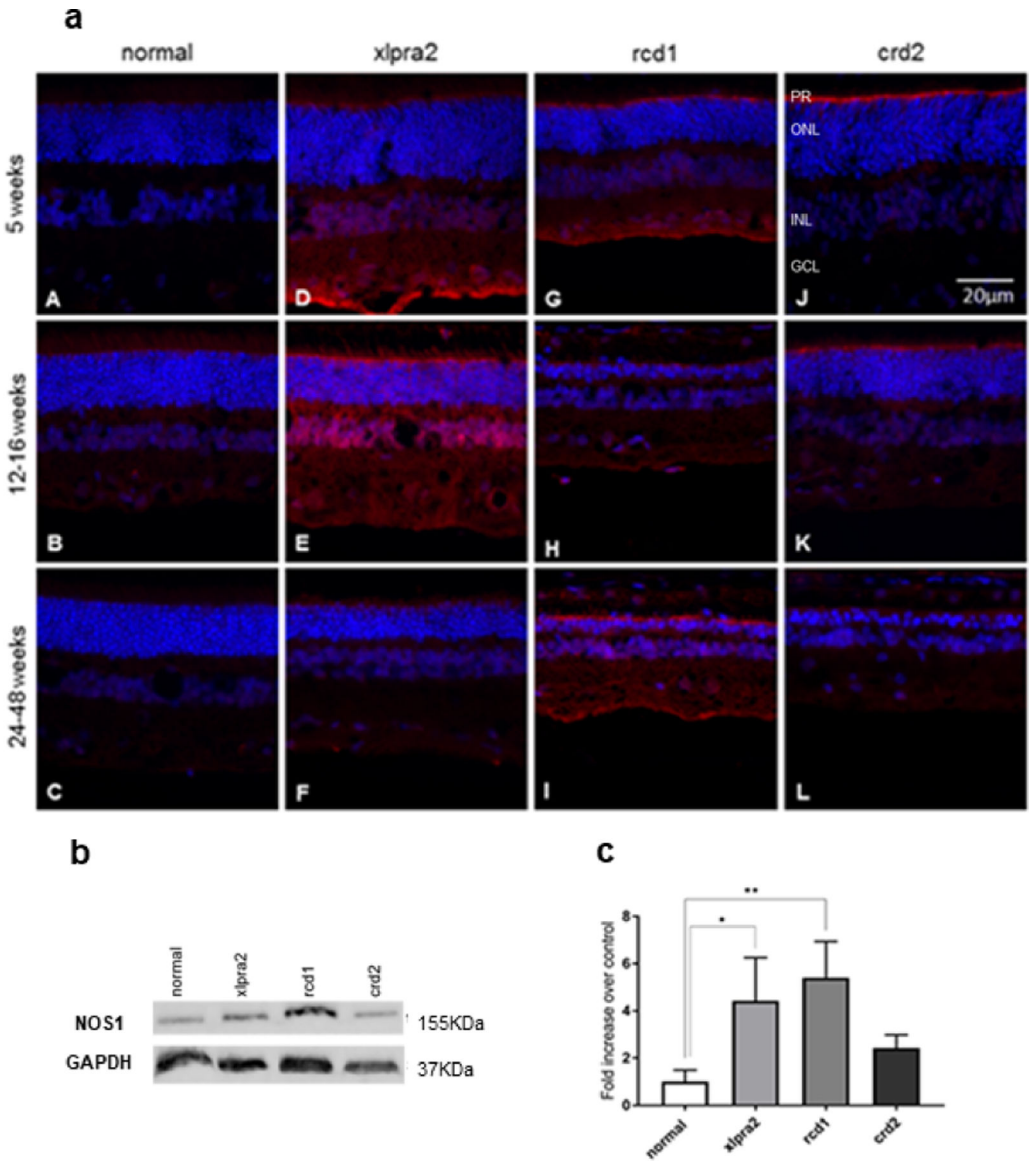


**Figure 5.**

Immunohistochemical (a) western blot (b), and densitometry analysis (c) of NOS1 expression in normal and mutant retinas. (a) NOS1 expression was not detected in the normal retina (A-C), while this protein (red fluorescence) was distinctly expressed in mutant retinas (D-L). There is increased immunolabeling in the inner segment region adjacent to the outer limiting membrane (OLM). There was more intense and widespread immunolabeling of the retina in the xlpra2 retina (D, E) and rcd1 (I). DAPI (blue) nuclear stain. Scale bar: 20 μm; PR: Photoreceptor cells, ONL: outer nuclear layer; INL: inner nuclear layer; GCL: ganglion cell layer. (b) western blot analysis of retinal samples taken in 7.7–13.6 weeks of age time window (see Table 1) with an antibody against NOS1. Equal sample loading was determined with a GAPDH internal control. (c) Normalized NOS1 protein expression as fold increase over normal samples. NOS1 protein levels in the xlpra2 and rcd1 retinas were increased significantly. The results are shown as the means ± SD. The significance of

difference among groups was evaluated by a one-way ANOVA with a post hoc ‘Tukey’s test. (One-way ANOVA, *P < 0.05).

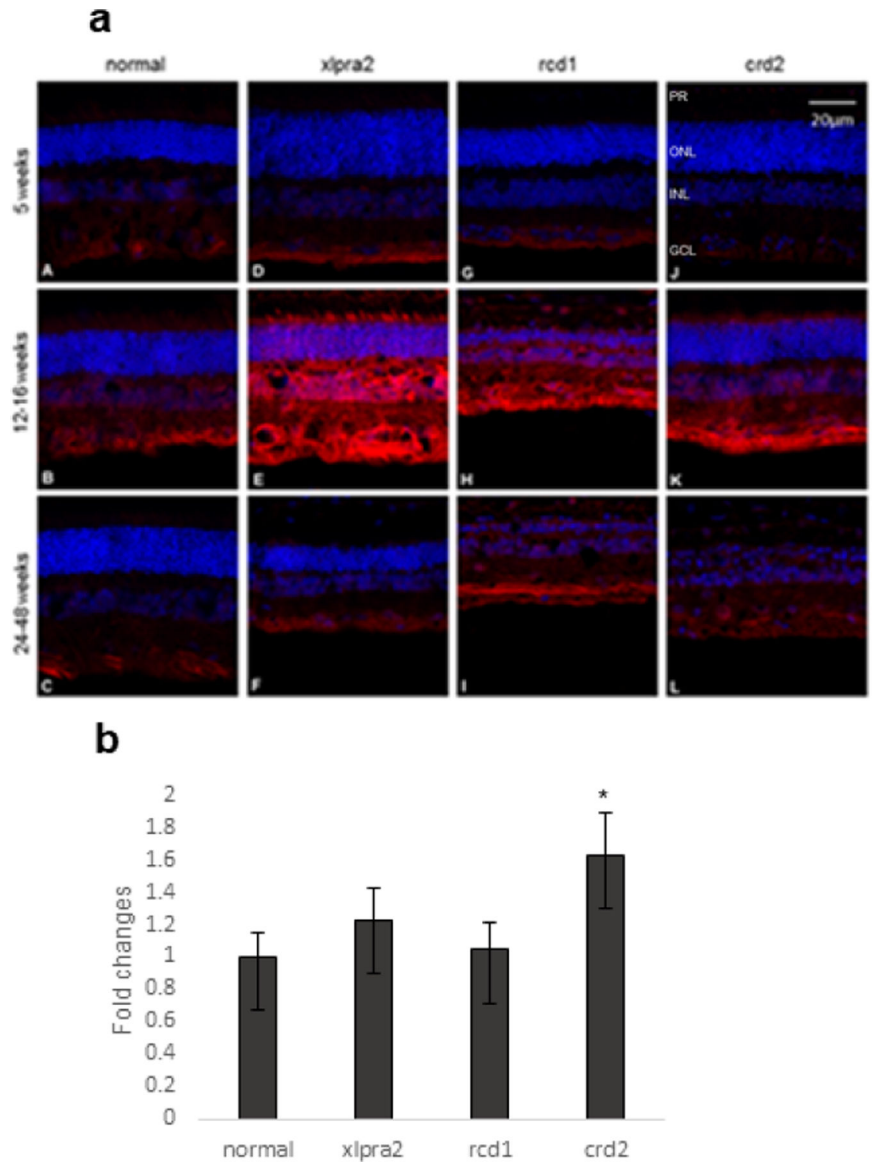


**Figure 6.**

Immunohistochemical (a) and mRNA (b) expression of NOS2 in normal and mutant retinas. (a) At a young age, NOS2 is expressed (red fluorescence) mainly in the GCL in normal and mutant retinas (A, D, G, J). At the time of active degeneration (E, H, K), immunolabeling intensity increases and is more intense in the nuclear and plexiform layers. This decreases after photoreceptor degeneration has progressed, and labeling is mainly restricted to the GCL (F, I, L). DAPI (blue) nuclear stain. Scale bar: 20 μm; PR: Photoreceptor cells, ONL: outer nuclear layer; INL: inner nuclear layer; GCL: ganglion cell layer. (b) NOS2 mRNA expression was normalized with GAPDH gene and expressed as fold change. The results showed that there was a significant increase in NOS2 expression in crd2 groups.

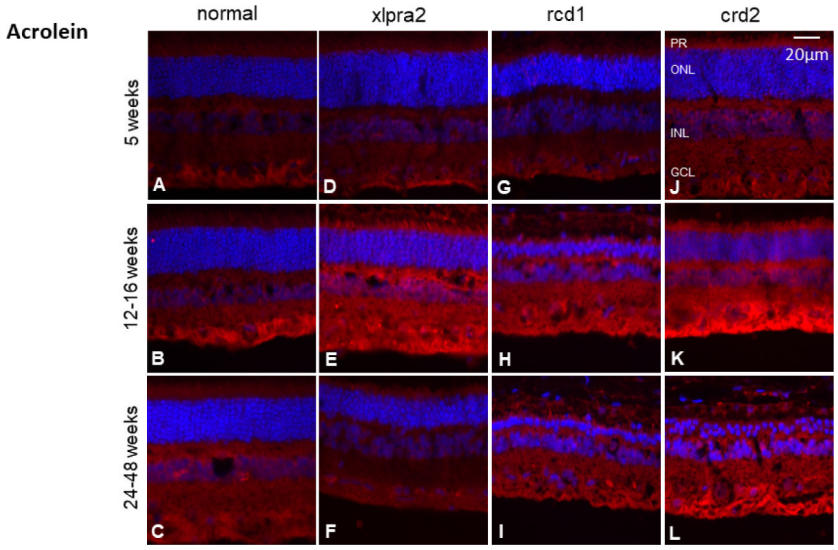


**Figure 7.**

Immunohistochemical (a and b), western blot (c), and densitometry analysis (d) of 4HNE expression in normal and mutant retinas. Figure (a) is the full image of the retina and figure (b) shows the higher magnification images that focus on the photoreceptors. HNE labeling (red fluorescence) is present in the photoreceptor layer in normal and mutant retinas. Inner segment labeling increases in intensity at the time of active degeneration (E, H, K) and remains elevated until photoreceptor inner and outer segments are lost (L). DAPI (blue) nuclear stain. Scale bar: 20 µm; PR: Photoreceptor cells, ONL: outer nuclear layer; INL: inner nuclear layer. (b) western blot analysis of retinal samples taken in 7.7–13.6 weeks of age time window (see Table 1) with an antibody against 4HNE. Equal sample loading was determined with a GAPDH internal control. (c) Normalized 4HNE protein expression as fold increase over normal samples. 4HNE protein levels were increased in the 3 mutant groups and were significant in the xlpra2 and rcd1 retinas. The results are shown as the means ± SD. The significance of difference among groups was evaluated by a one-way ANOVA with a post hoc Tukey's test. (One-way ANOVA, *P < 0.05).

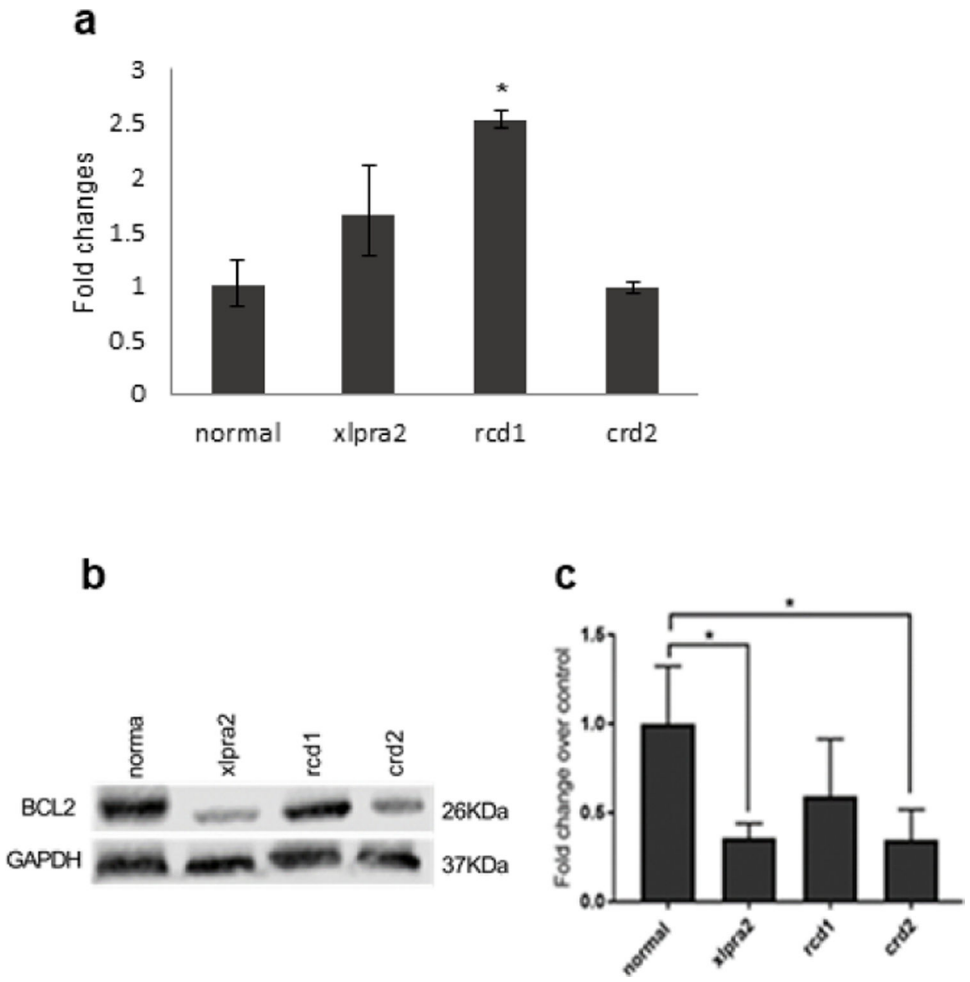


**Figure 8.**

Immunohistochemical analysis of acrolein expression (red fluorescence) in normal and mutant retinas. At the time of active degeneration, there was a retina-wide increase in acrolein expression (E, H, K). After photoreceptor degeneration is almost completed, intensity decreases but remains elevated in rcd1 and crd2 retinas (I, L). DAPI (blue) nuclear stain. Scale bar: 20 μm; PR: Photoreceptor cells, ONL: outer nuclear layer; INL: inner nuclear layer; GCL: ganglion cell layer.

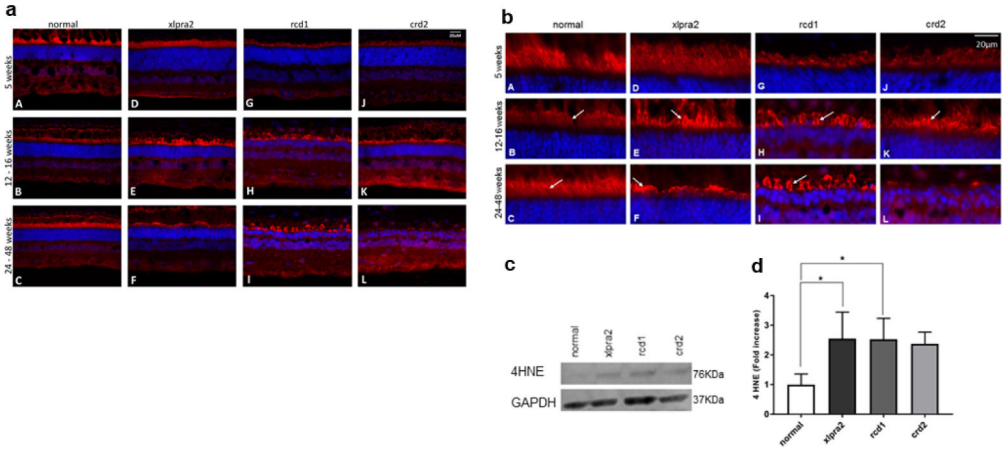


**Figure 9.**

qRT-PCR (a), western blot (b), and densitometry analysis (c) of BCL2 expression in normal and mutant canine retinal samples taken in 7.7–13.6 weeks of age time window (see Table 1). (a) mRNA expression, normalized to GAPDH, showed increased expression in xlpra2 and rcd1, and the increase was significant in rcd1. (b, c) western analysis with an anti BCL2 antibody. (c) Normalized BCL2 protein expression as fold increase over normal samples normalized with a GAPDH internal control. BCL2 protein levels are decreased in the 3 different mutant retina groups, significant in xlpra2 and crd2. The significance of difference among groups was evaluated by a one-way ANOVA with a post hoc Tukey's test. (One-way ANOVA, *P < 0.05).

**Table 1.**

The number, age in weeks, and the gender (Male or Female) of the animals used for this study.

| Animals | qPCR | WB | IHC |
|---|---|---|---|
| Normal | 7.7–11.7 (n=3; 2F, 1M) | 7.7–11.7 (n=3; 2F, 1M) | 5, 12 and 48 (n=3; 1F, 2M) |
| Xlpra2 | 12–12.4 (n=3; 3F) | 12–12.4 (n=3; 3F) | 5,12 and 24 (n=3; 3F) |
| rcd1 | 8.6–13.6 (n=3; 3M) | 8.6–13.6 (n=3; 3M) | 5, 16 and 40 (n=3; 1M, 2F) |
| crd2 | 8.7 (n=3; 3M) | 8.7 (n=3; 3M) | 6, 14 and 42 (n=3; 3M) |

* The retina samples used for qRT-PCR (qPCR) and western blot (WB) analysis were collected from the same dogs.

**Table 2.**

PCR primer sequences, optimal amplification cycles, optimal annealing temperature, and product size

| Gene | Accession number | Primer sequence | Optimal condition |
|---|---|---|---|
| CSE | XM_537115 | F: 5-GCAATGGAATTCTCGTGCCG-3’<br>R: 5-ATGCAAAGGCCAAACTGTGC-3’ | 40 cycles Annealing 60°C |
| CBS | XM_014109845 | F: 5-GGCTGGAAAGGTGCGGCCAT-3’<br>R: 5-CTTGCTGGACATGCCATTGCTG | 40 cycles Annealing 60°C |
| NOS2 | NM_001313848.1 | F: 5-ACTTCTCCTGGCTGTCTCT-3’<br>R: 5-GGCCTACTGACTTCACTTATG-3’ | 40 cycles Annealing 60° |
| BCL2 | NM_001002949.1 | F: 5-ACTTCTCCTGGCTGTCTCT-3’<br>R: 5-GGCCTACTGACTTCACTTATGG-3’ | 40 cycles Annealing 60° |
| GAPDH | NM-001003142 | F: 5-CTGTCGAGTCGCGTCCACCC-3<br>R: 5-ACATGCCGGAGCCGTTGTCG-3’ | 40 cycles Annealing 60°C |

**Table 3.**

Antibodies used for western blot and immunohistochemistry.

| Antigen | Antibody | Host | Type | Immunogen species | Dilution for WB | Dilution for IHC |
|---|---|---|---|---|---|---|
| CBS | Proteintech, 14787–1-AP | Rabbit | IgG Polyclonal | Human | 1:1000 | 1:500 |
| CSE | Proteintech, 60234–1 -Ig | Mouse | IgG1 Monoclonal | Human | 1:1000 | 1:500 |
| NOS1 | Proteintech, 18984–1-AP | Rabbit | IgG Polyclonal | Human | 1:1000 | 1:200 |
| NOS2 | Novus NB300–605SS | Rabbit | IgG Polyclonal | Mouse | - | 1:200 |
| 4HNE | ALPHA DIAGNOSTIC INTERNATIONAL HNE11-S | Rabbit | IgG Polyclonal | Free HNE coupled with Keyhole limpet hemocyanin | 1:1000 | 1:200 |
| Acrolein | Novus NBP2–59359 | Mouse | IgG1 Monoclonal | Synthetic | - | 1:200 |
| GAPDH | Proteintech, 10494–1-AP | Rabbit | IgG Polyclonal | Human | 1:10000 | - |
| GAPDH | Proteintech, 60004–1-lg | Mouse | IgG2b Monoclonal | Human | 1:10000 | |